Dihydronicotinamide riboside is a potent NAD^+ concentration enhancer *in vitro* and *in vivo*

Received for publication, September 8, 2018, and in revised form, March 31, 2019 Published, Papers in Press, April 4, 2019, DOI 10.1074/jbc.RA118.005772

Yue Yang, Farheen Sultana Mohammed, Ning Zhang, and Anthony A. Sauve[1]

From the Department of Pharmacology, Weill Cornell Medical College, New York, New York 10065

Edited by Jeffrey E. Pessin

Interest in pharmacological agents capable of increasing cellular NAD^+ concentrations has stimulated investigations of nicotinamide riboside (NR) and nicotinamide mononucleotide (NMN). NR and NMN require large dosages for effect. Herein, we describe synthesis of dihydronicotinamide riboside (NRH) and the discovery that NRH is a potent NAD^+ concentration-enhancing agent, which acts within as little as 1 h after administration to mammalian cells to increase NAD^+ concentrations by 2.5–10-fold over control values. Comparisons with NR and NMN show that in every instance, NRH provides greater NAD^+ increases at equivalent concentrations. NRH also provides substantial NAD^+ increases in tissues when administered by intraperitoneal injection to C57BL/6J mice. NRH substantially increases NAD^+/NADH ratio in cultured cells and in liver and no induction of apoptotic markers or significant increases in lactate levels in cells. Cells treated with NRH are resistant to cell death caused by NAD^+-depleting genotoxins such as hydrogen peroxide and methylmethane sulfonate. Studies to identify its biochemical mechanism of action showed that it does not inhibit NAD^+ consumption, suggesting that it acts as a biochemical precursor to NAD^+. Cell lysates possess an ATP-dependent kinase activity that efficiently converts NRH to the compound NMNH, but independent of Nrk1 or Nrk2. These studies identify a putative new metabolic pathway to NAD^+ and a potent pharmacologic agent for NAD^+ concentration enhancement in cells and tissues.

NAD^+ metabolism is largely composed of biosynthetic, redox-active, and "NAD^+-consuming" pathways (1, 2). In biosynthetic pathways, NAD^+ is made from different NAD^+ precursors. In redox-active pathways, NAD^+ is used to conduct hydride equivalents between reductants and oxidants. In NAD^+-consuming pathways, NAD^+ is consumed via enzymes that transfer the ADP-ribose moiety to cellular nucleophiles (3, 4). Reactions in each group are plentiful in cells, making NAD^+ one of the most versatile of cellular metabolites. NAD^+ is required in abundant amounts, existing at concentrations of 100–500 μM in most mammalian cells and tissues (see Table 1 for examples) (5). NAD^+ metabolism has become a topic of renewed interest in recent years (6), notably focused upon the involvement of ADP-ribose transfer/sirtuin deacylation reactions in mediating key cellular processes (7), such as DNA repair (8), metabolic adjustment (8), apoptosis (5), cell survival (6), stem cell fitness (6, 9), and even lifespan regulation (9–11).

The substrate role of NAD^+ for key signaling enzymes has sparked investigations to determine whether increased NAD^+ concentrations provide an impetus for cellular changes. Of interest are genetic or pharmacologic interventions that can significantly alter NAD^+ concentrations, probing for downstream effects mediated by ADP ribosyltransferases/sirtuins. This work has provided evidence that increased NAD^+ concentrations drive signaling programs leading to key biochemical processes, such as enhanced mitochondrial biogenesis (12), protection against fatty acid–induced liver disease (13), improved exercise performance (14), and reduced neurodegeneration (15, 16), in a variety of animal models. In turn, these results have turned attention to nicotinamide riboside (NR)[2] (17–19) and nicotinamide mono-nucleotide (NMN) (18, 19) as possible NAD^+ precursors, with findings that these agents are promising for raising cellular and tissue NAD^+ concentrations. Very recently, a number of clinical studies of these agents in humans have been published (20–22), confirming their activities as NAD^+ concentration boosters in humans and setting the stage for further development as human therapeutics (1, 6).

There are limitations of the current set of NAD^+ concentration enhancers, including maximal reported cellular effects for NAD^+ enhancement of 270% (17) and requirements of high doses to achieve beneficial effects in animal models of disease with reported doses typically 250–1000 mg/kg in mice (14, 23, 24). These limitations stimulated our laboratory to investigate other chemical structures related to NR and NMN as possible NAD^+ precursors. Of interest to us was dihydronicotinamide riboside (NRH), which has never been investigated as a precursor in NAD^+ metabolism, to our knowledge. Interestingly, an enzymatic activity that preferentially uses NRH as a substrate

This work was funded in part by National Institutes of Health Grant GM R01-106072 (to A. A. S.) and New York Spinal Cord Research Board Contract C32098GG (to A. A. S.). The authors A. A. Sauve, Y. Yang, and F. Sultana Mohammed have filed a patent on aspects of this work in conjunction with Cornell University. A. A. Sauve has intellectual property related to NR and derivatives of NR. Chromadex Inc. (Irvine, CA) has a license on intellectual property related to production and uses of NR. A. A. Sauve is a consultant and a co-founder of Metro MidAtlantic Biotech LLC and Metro International Biotech LLC. The content is solely the responsibility of the authors and does not necessarily represent the official views of the National Institutes of Health.

This article contains Figs. S1–S5.

[1] To whom correspondence should be addressed. Tel.: 212-746-6224; E-mail: aas2004@med.cornell.edu.

[2] The abbreviations used are: NR, nicotinamide riboside; NMN, nicotinamide mononucleotide; NRH, dihydronicotinamide riboside; NMNH, dihydronicotinamide mononucleotide; HP, hydrogen peroxide; MMS, methylmethane sulfonate; NAM, nicotinamide; Nampt, nicotinamide phosphoribosyltransferase; KO, knockout.

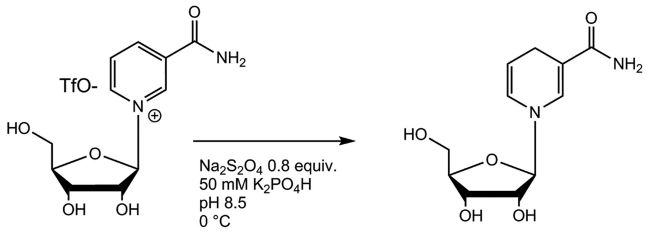

Nicotinamide riboside triflate — **Dihydronicotinamide riboside "NRH"**

Scheme 1. Synthesis of NRH from nicotinamide riboside triflate.

had been characterized previously. The enzyme NQO2, a quinoneoxidoreductase, is known to use NRH preferentially as the upstream reductant, in a reaction that converts quinones to dihydroquinones (25, 26). However, the effects of NRH in altering cellular NAD$^+$ levels have remained unexamined in the published literature. In this paper, we report properties of NRH as an enhancer of cellular NAD$^+$ concentrations. NRH is effective in this respect in mammalian cells and in mice tissues. NRH acts at concentrations equal to or lower than those observed for NR and NMN and surpasses NR and NMN in biological effect *in vitro* and *in vivo*. We identify a putative biochemical mechanism of action wherein NRH represents a starting point for a novel biosynthetic pathway to NAD$^+$.

Results

Preparation of NRH

To better investigate the properties of NRH (Scheme 1) as a potential NAD$^+$ precursor, a method of preparation of the compound was required, preferably by direct chemical synthesis. We prepared the compound from nicotinamide riboside triflate, via published synthetic methodology developed by our laboratory (17). NR (triflate) was reduced in aqueous solution in 50 mM potassium phosphate, pH 8.6, with 0.80 eq of sodium dithionite, followed by immediate purification on C-18 resin to provide purified NRH (Scheme 1; see "Experimental procedures"). The ^{1}H NMR spectrum agreed with a prior literature report for this compound (see supporting information for ^{1}H NMR and ^{13}C NMR spectra). Additional properties of NRH are provided in the supporting information, including its UV spectrum, which is centered at 340 nm (see Fig. S1). The compound is strongly fluorescent (excitation wavelength = 340 nm), similar to NADH. NRH has moderate chemical stability at pH values below 7, with a half-life of decomposition of 3 h at 37 °C at pH 6.0 (Fig. S2). Consequently, only freshly prepared NRH solutions were used in all experiments.

NAD$^+$ concentration increases caused by exposure to NRH

To assess whether NRH can be absorbed by cells and change NAD$^+$ concentrations, we exposed a number of mammalian cell lines, including insulinogenic (INS1 and MIN6), neuron-like (F98, U87, and LN229), muscle-like (C2C12), and HEK293 cells with vehicle, 1 mM NR, or 1 mM NRH for time periods of 6 h. Cellular NAD$^+$ concentrations were determined in accord with our published assay (27). Changes in NAD$^+$ concentrations were 2.4–10-fold for cells exposed to NRH, well above levels reported for any other NAD$^+$ precursor yet studied (Fig. 1*a*). In each cell line, NRH exceeded the NAD$^+$ concentration enhancement caused by NR by at least 2-fold and in all cases greatly exceeded the levels induced by NMN (see Fig. S3). These data establish that NRH is effective in stimulating NAD$^+$ increases in cultured mammalian cells superior to NR or NMN. To further confirm the NAD$^+$ enhancement effect of NRH, we examined an additional neuron-derived cell line (Neuro2a) treated with NRH, which caused an ~10-fold increase in NAD$^+$ concentrations compared with control (Fig. 1*b*), an enhancement for an NAD$^+$ precursor that is unprecedented to our knowledge. To unequivocally confirm increased NAD$^+$ production, lysate obtained from Neuro2a cells treated for 6 h with NRH was analyzed using HPLC to directly detect the increased NAD$^+$ amount using an untreated control as a comparison and employing an NAD$^+$ standard to confirm identity. As shown in Fig. 1*c*, NRH substantially increased the peak corresponding to NAD$^+$ by manyfold in the NRH-treated lysate mixture, well above the level for control. To validate our other NAD$^+$ measurements, we checked for possible interference of NRH in the plate reader assay typically employed (27), but minimal interference from NRH was observed when the assay was performed at relevant NRH concentrations (see supporting information for details). Thus, we can conclude by two independent assays (HPLC and plate reader NAD$^+$ assay) that NAD$^+$ concentrations are substantially increased by NRH exposure to cultured mammalian cells.

A dose-response profile for NRH on NAD$^+$ concentration was obtained in Neuro2a cells. Concentrations of NRH in medium were varied from 100 to 2000 μM for a period of 6 h. NAD$^+$ concentration increase reached greater than 10-fold (Fig. 2*a*). Maximal NAD$^+$ increase was determined by theoretical fit of the curve,

$$[NAD^+] = B_{max}[NRH]/([NRH] + EC_{50}) + B_0 \qquad \text{(Eq. 1)}$$

where B_{max} is maximum biological effect caused by NRH, EC_{50} is the concentration to achieve 50% of B_{max}, and B_0 is the untreated control NAD$^+$ concentration. The values obtained were B_{max} = 11,200 pmol/10^6 cells, and EC_{50} was found to be 310 μM. The value for B_0 was 690 pmol/10^6 cells. According to the curve, the concentration of NRH required to achieve 260% NAD$^+$ concentration increase as compared with control was determined to be 34 μM, whereas 1 mM NR is required to achieve the same increase in this cell line (17), and NMN does not achieve doubling of NAD$^+$ concentration at 1 mM (Fig. S3). These data provide a relative potency increase of ~30-fold *versus* NR for this cell line. A dose-response profile was also determined for primary neurons, obtained as described previously (28). These cells were treated with increasing concentrations of NRH for a period of 6 h. At the lowest concentration of NRH tested, 100 μM, neuronal NAD$^+$ concentrations were ~5-fold elevated over corresponding controls, and saturation was reached at 500 μM, where concentrations reached 7.5-fold over untreated controls. To further investigate whether NRH can alter subcompartment NAD$^+$ concentrations, we measured mitochondrial NAD$^+$ content, which is known to increase with some NAD$^+$ concentration enhancers, such as NR (14). This compartment had increased NAD$^+$ concentrations of at least

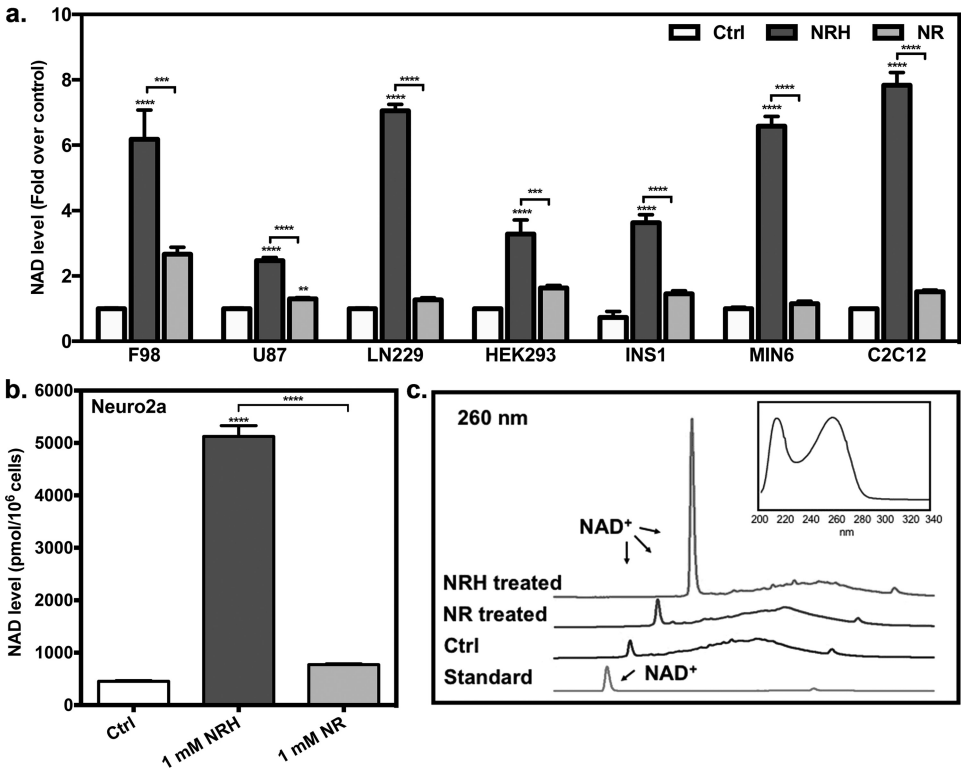

Figure 1. NAD$^+$ increases in different mammalian cell lines. *a*, F98, U87, LN229, HEK293, INS1, MIN6, and C2C12 cells were treated with either 1 mM NRH or 1 mM NR for 6 h. Their cellular NAD$^+$ changes are expressed as -fold over control. Data are expressed as mean ± S.E. (*error bars*) ($n = 6$). *b*, NRH induces NAD$^+$ increase in Neuro2a cells. The cellular NAD$^+$ content of Neuro2a cells treated with either 1 mM NRH or 1 mM NR for 6 h is shown. Data are expressed as mean ± S.E. ($n = 4$). ****, $p < 0.0001$. *c*, NAD$^+$ peaks in HPLC chromatograms of control Neuro2a cell lysates or cell lysates treated with 1 mM NRH or 1 mM NR. The absorbance is shown at 260 nm. *Top right*, representative spectrum of NAD$^+$ peak.

3.5-fold in Neuro2a cells treated with NRH at 1 mM after 18 h (Fig. 2*c*).

Time courses for NRH action were also performed. Thus, Neuro2a cells and HEK293 cells were treated with NRH for different incubation times and then harvested, and NAD$^+$ contents were assayed. We determined that the NAD$^+$ concentration-elevating effects were present as early as 1 h in HEK293 cells, with full effects evident at 6 h (Fig. 2*d*). We saw a similar strong effect in Neuro2a cells at 6 h (Fig. 2*e*). Robust NAD$^+$ elevation caused by treatment of NRH remained evident after 18 h in HEK293 cells (Fig. 2*d*), in part due to persistence of the majority NRH in medium past a time of 18 h (Fig. S2).

Lack of toxicity and rescue effects in genotoxicity

These large increases in NAD$^+$ concentrations caused us to wonder about possible toxicity to cells. We did not observe any appreciable loss of cells in culture from exposure to 1 mM NRH for 24 h (Fig. S4). For example, cell counts were similar between controls and NRH-treated cells for Neuro2a, although cell counts were slightly lower in HEK293 cells after 24 h. Trypan blue–positive cells were similar in both cases, not exceeding 3%, and there were no significant differences in apoptotic markers. Annexin V or caspase-3/7 in NR- and NRH-treated cells *versus* controls, indicating no changes in apoptotic pathway activation (Fig. S4).

NRH is a reductant, and we considered that it could potentially cause changes to the NAD$^+$/NADH ratio. Thus, we measured the ratio after NRH treatment. NAD$^+$/NADH ratio is regulated in cells and is typically highly oxidizing under most physiological conditions (29). However, the effect on this ratio upon increasing NAD$^+$ concentrations up to 10-fold from resting levels has not been assessed, to our knowledge. Thus, we treated cells for 6 h with NRH and measured NAD$^+$ concentration and NADH concentration independently (27) to determine absolute amounts of NAD$^+$ and absolute amounts of NADH. We found that NAD$^+$ concentrations were substantially increased as expected, but NADH concentrations were not increased proportionally (Fig. 2*e*). Thus, a consistent effect of NRH treatment is a net increase in the NAD$^+$/NADH ratio in four different mammalian cell lines (Fig. 2*f*). Interestingly, Cantó *et al.* (14) reported that NR-induced NAD$^+$ increase in animal tissues caused an increased NAD$^+$/NADH ratio. As another way to identify perturbation in NAD$^+$/NADH ratio, we measured lactate concentrations in cell culture. Both intracellular lactate levels and extracellular lactate were measured at a time of 6 h. We saw no statistically significant increases in lactate in medium, and intracellular lactate levels were largely unaffected, except in one instance, where intracellular lactate was substantially depleted within HEK293 cells (Fig. S5). The preceding results showed that millimolar concentrations of NRH are well-tolerated by cells and that highly elevated NAD$^+$ levels are well-tolerated and do not lead to obvious toxic effects, at least over a 24-h period.

Intrigued by the magnitude of NAD$^+$ concentration enhancement, we wondered whether NRH could improve cell

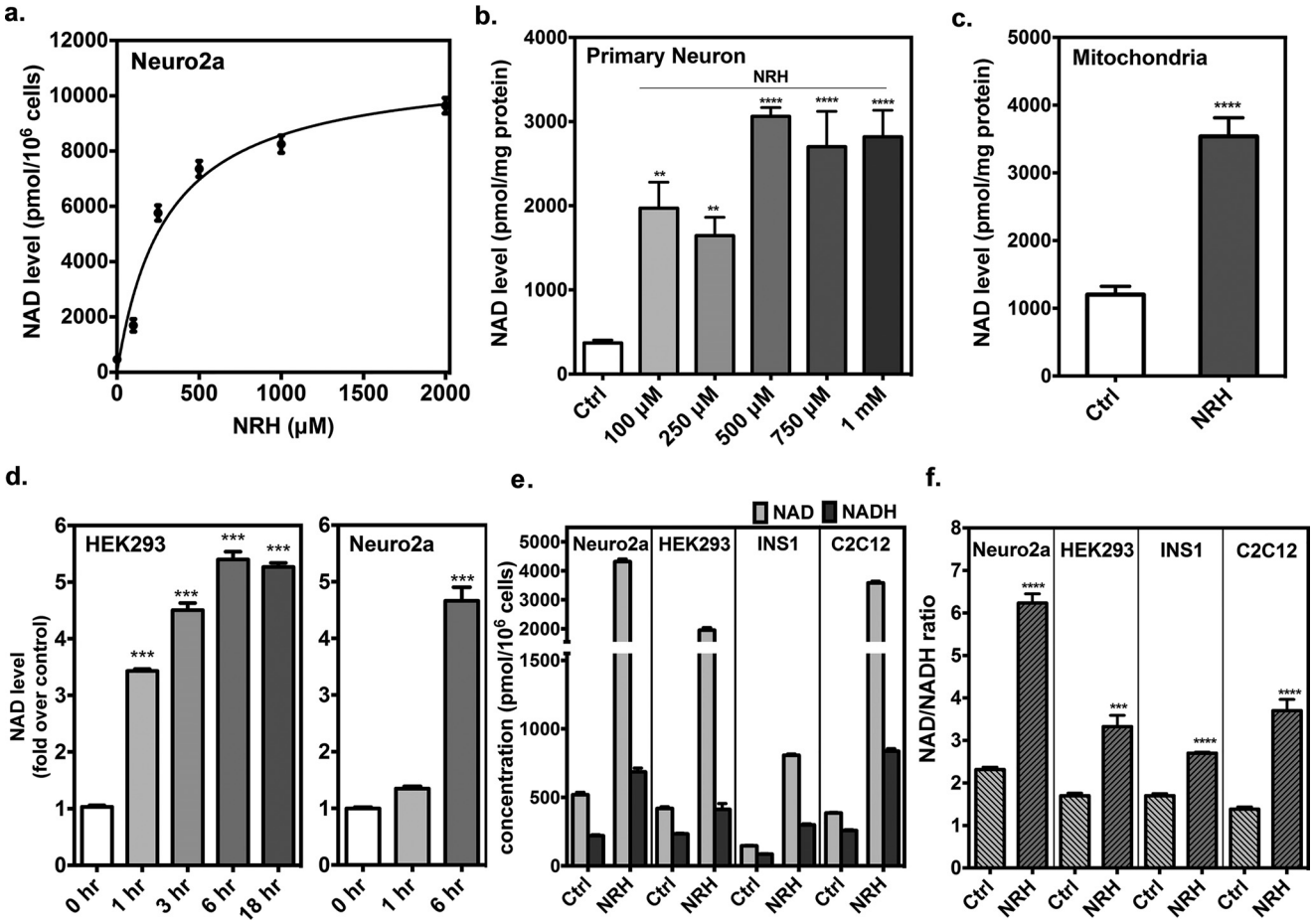

Figure 2. Effects of NRH in different scenarios. *a*, dose-response of NRH in Neuro2a cells. Neuro2a cells were incubated with 100, 200, 500, 1000, and 2000 μM for 6 h. Fit is described under "Results." *b*, dose-response of NRH in primary neurons extracted from neonatal rat brains. Primary neuron cells were incubated with 100, 250, 500, 750, and 1000 μM NRH for 6 h. *c*, mitochondrial NAD$^+$ contents in Neuro2a cells treated with 1 mM NRH for 18 h. Data are expressed as mean ± S.E. (*error bars*) ($n = 4$). *d*, NRH increased NAD$^+$ levels in a time-dependent manner in HEK293 and Neuro2a cells. HEK293 cells were incubated with 1 mM NRH for 1, 3, 6, and 18 h. Neuro2a cells were incubated with 1 mM NRH for 1 and 6 h. Data are expressed as mean ± S.E. ($n = 4$). *e*, NAD$^+$ and NADH values were measured side by side in Neuro2a, HEK293, INS1, and C2C12 cells treated with 1 mM NRH for 6 h. *f*, NAD$^+$/NADH ratios. Data are shown as mean ± S.E. ($n = 4$). *, $p < 0.05$; **, $p < 0.01$; ***, $p < 0.001$; ****, $p < 0.0001$.

survival under stressful conditions that deplete NAD$^+$. Thus, we examined genotoxicity, which causes DNA damage and activates poly(ADP-ribose) polymerases and causes NAD$^+$ depletion (30). Strong genotoxicity can lead cells to severely deplete NAD$^+$, leading to cell death (5). Thus, we treated Neuro2a cells with hydrogen peroxide (HP) for a period of 6 h and then counted cells and measured NAD$^+$ in samples co-treated either with NRH (1 mM) or with vehicle. We found that cell survival improved from 10% (HP) to nearly 80% with HP + NRH treatment (Fig. 3*a*). In addition, NAD$^+$ levels remained highly elevated in HP + NRH–treated cells, whereas in HP cells, NAD$^+$ concentrations became substantially depleted below control values (Fig. 3). Similar results were obtained with INS1 cells, which are insulin-containing cells and sensitive to HP. Cell survival went completely to zero in HP treatment but was increased to nearly 50% in HP + NRH (Fig. 3*b*). We then compared NR effects with NRH in Neuro2a cells at a lower concentration of 250 μM and found that NRH is still protective of not only NAD$^+$ level but cell survival, whereas, although NR treatment is also effective, it does so much less well, in both preservation of NAD$^+$ content and cell viability (Fig. 3*c*).

To broaden these findings, we examined the alkylative genotoxin methylmethane sulfonate (MMS), which we have used in past studies (5), on Neuro2a and HEK293 cells. Cell survival in Neuro2a cells improved with NRH co-treatment with MMS, with survival reaching near 100%, indicating full protection in MMS + NRH–treated samples. NAD$^+$ concentrations plummeted in this case, to below untreated control value, but were still higher than MMS treatment alone (Fig. 3*d*). In HEK293 cells, survival was improved considerably from 20% (MMS) to nearly 80% (MMS + NRH; Fig. 3*e*). Furthermore, MMS + NRH treated cells had higher NAD$^+$ concentrations *versus* MMS treatment alone. Thus, challenge to cells with genotoxicity identifies conditions where NRH substantially improves cell survivability, concurrently protecting the cellular NAD$^+$ pool from depletion. Again, we compared NR with NRH at 250 μM (Fig. 3*f*) and found that NR could not provide protection of cells at this concentration and only modestly improved NAD$^+$ levels *versus* untreated controls, whereas NRH provided statistically significant increases in cell survival as well as increased NAD$^+$ concentrations *versus* corresponding MMS-treated control.

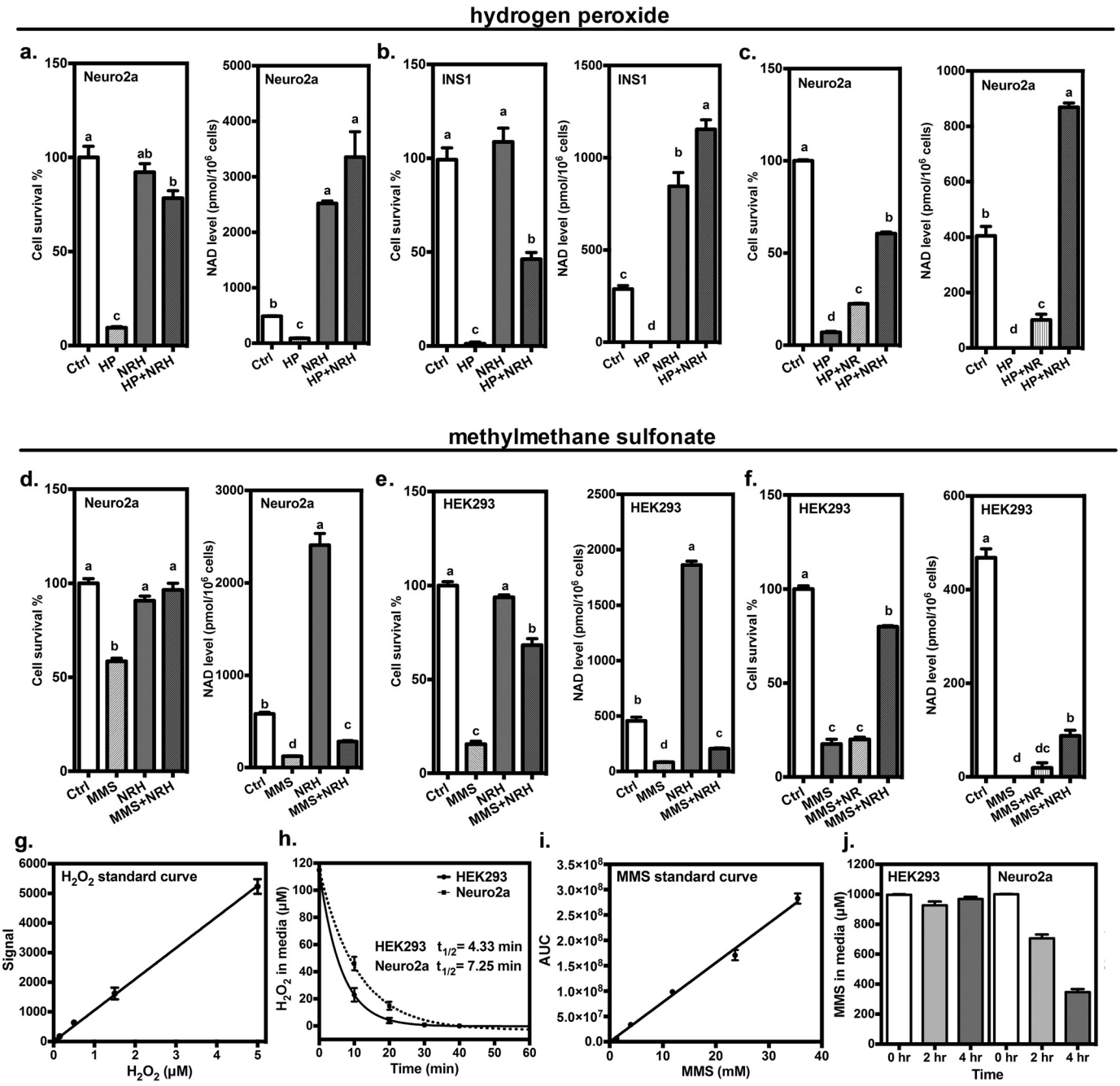

Figure 3. NRH protects cells from genotoxicity. Neuro2a cells (*a*) and INS1 cells (*b*) were exposed to 500 μM HP with or without the co-incubation of 1 mM NRH for 6 h. *c*, Neuro2a cells were treated with 500 μM HP in the presence of either 250 μM NR or NRH for 6 h. Neuro2a cells (*d*) and HEK293 cells (*e*) were treated with 400 μM MMS with or without the co-incubation of 1 mM NRH for 6 h. *f*, HEK293 cells were treated with 400 μM MMS, with or without 250 μM NR or NRH. Their survival rate and cellular NAD$^+$ content are expressed as mean ± S.E. (*error bars*) ($n = 4$). *Different letters* indicate significant difference ($p < 0.05$) between groups. *g*, standard curve constructed with different concentrations of HP. *h*, stability of 100 μM HP in medium with cultured cells. *Solid curve*, HEK293 cells; *dashed curve*, Neuro2a cells. Fit provided *k* values of 0.094 min^{-1} for Neuro2a cells and 0.160 min^{-1} for HEK293 cells. Maximal rate under the assay conditions was determined to be 9.4 μM min^{-1} at 100 μM for Neuro2a cells and 16 mM min^{-1} for HEK293 cells, corresponding to a half-life of 7.25 min for Neuro2a cells and 4.33 min for HEK293 cells. *i*, HPLC assay to quantify MMS concentration and resulting standard curve. *j*, amount of MMS left in medium quantified with initial 1 mM MMS combined with HEK293 and Neuro2a cells at 0, 2, and 4 h.

The differences in NAD$^+$ concentrations observed at 6 h in cells for the two genotoxins appear to arise from differing lifetimes of the genotoxins in cell culture. Peroxide is depleted rapidly in cell culture (see standard curve and depletions in Fig. 3 (*g* and *h*, respectively)). Rapid depletion of peroxide allows rebound to the NAD$^+$ concentrations in NRH-treated cells at 6 h. On the other hand, MMS persists in cell culture past 6 h (see standard curve and depletions in Fig. 3 (*i* and *j*, respectively)). This stability explains persistent depletion of NAD$^+$ concentrations at harvest, even in NRH-treated cells.

Possible biochemical mechanisms of NRH-induced increases to NAD$^+$

To better understand the possible mechanisms where NRH exposure to cells causes NAD$^+$ concentrations to accumulate, we sought to determine whether NAD$^+$ turnover is inhibited by

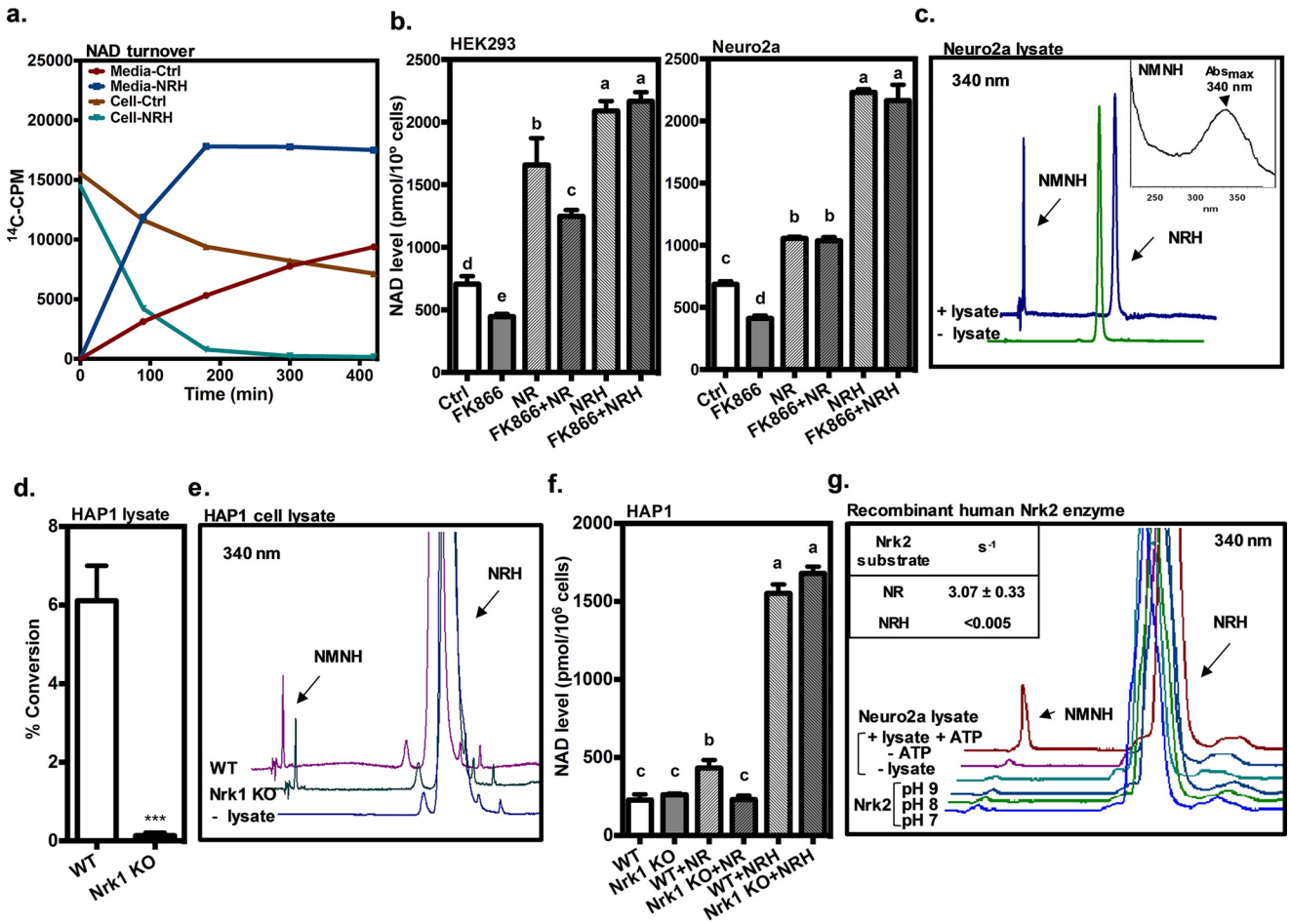

Figure 4. NRH conversion to NAD$^+$ via a kinase mechanism. *a*, NAD$^+$ turnover in Neuro2a cells treated with or without NRH. Neuro2a cells were incubated with [*carbonyl*-^{14}C]nicotinamide overnight and then treated with or without 1 mM NRH. Radioactivity was counted in both medium, and NAD$^+$ was purified and counted at 0, 90, 180, 300, and 420 min after the treatment. *b*, FK866 did not inhibit the NAD$^+$-raising effect of NRH. HEK293 and Neuro2a cells were treated with the Nampt inhibitor FK866 or vehicle with or without 1 mM NR or NRH for 6 h. Data are expressed as mean ± S.E. ($n = 4$). *Different letters* indicate significant difference ($p < 0.05$) between groups. *c*, NRH is converted to NMNH by cell lysate. After incubation with Neuro2a protein lysate for 30 min at 37 °C, a new peak, detected at 340-nm wavelength on HPLC chromatography, is identified as NMNH. Conditions are described under "Experimental procedures." *Inset*, UV spectrum for this product. *d*, protein lysate from WT HAP1 cells can convert [*carbonyl*-^{14}C]NR into [*carbonyl*-^{14}C]NMN, but the activity has been abolished in lysate from human Nrk1 knockout HAP1 cells. *e*, when using NRH as substrate, both lysates from WT and human Nrk1 knockout HAP1 cells generate NMNH. *f*, WT and human Nrk1 knockout HAP1 cells were treated with either 1 mM NR or NRH for 6 h and measured for NAD$^+$ content. Data are expressed as mean ± S.E. (*error bars*) ($n = 4$). *Different letters* indicate significant difference ($p < 0.05$) between groups. *g*, Neuro2a protein lysate produced NMNH from NRH in the presence of ATP. When using recombinant human Nrk2 protein in the reaction carried out in pH 7, 8, and 9 buffers, no significant NMNH peak could be observed at 340 nm. The activity of recombinant human Nrk2 was validated using [*carbonyl*-^{14}C]NR as substrate and compared with NRH activity quantified in the *inset*.

NRH treatment. Therefore, we treated cells with [*carbonyl*-^{14}C]nicotinamide (NAM), which becomes converted to [*carbonyl*-^{14}C]NAD$^+$ in cells as shown by HPLC (0 time; Fig. 4*a*). After washing cells of residual radioactivity in medium, we exposed labeled cells to NRH or vehicle and measured intracellular labeled NAD$^+$ as a function of time using HPLC and scintillation counting. Extracellular radioactivity in the form of released [*carbonyl*-^{14}C]NAM was also determined at each time point. Time-dependent outcomes of the experiment (NRH *versus* control) are expected as follows: 1) no change in loss of label at each time for NRH-treated samples is indicative of no inhibition of turnover by NRH; 2) increased loss of label at each time for NRH samples is indicative of increased NAD$^+$ turnover and no inhibition of turnover by NRH; and 3) decreased label loss at each time for NRH samples is indicative of inhibition of NAD$^+$ turnover by NRH. Radiolabeled NAD$^+$ acts as a reporter for the entire NAD$^+$ pool, as there is no expected isotope effect on turnover for a *carbonyl*-^{14}C label. Exposure of radiolabeled Neuro2a cells with 1 mM NRH resulted in rapid loss of label from NAD$^+$, with a half-life of less than 100 min (Fig. 4*a*), whereas corresponding controls not exposed to NRH lose label to NAD$^+$ with an approximate half-life of 240 min (Fig. 4*a*). Corresponding release of radioactivity to medium is correlated to label loss (Fig. 4*a*). Thus, exposure of cells to NRH accelerates radiolabel loss from intracellular NAD$^+$, which is consistent with increased NAD$^+$ reaction and degradation (*i.e.* NAD$^+$ consumption). This result provides evidence that NRH does not inhibit NAD$^+$ turnover. Thus, inhibition of NAD$^+$ consumption does not obviously contribute to NRH-induced NAD$^+$ concentration increase.

Increased NAD$^+$ consumption in the presence of NAD$^+$ accumulation in cells suggests that NRH causes a marked increase in NAD$^+$ biosynthesis. Because NRH provides a substantially higher accumulation effect than for other NAD$^+$ precursors, it suggests possible involvement of multiple biosynthetic pathways converging to NAD$^+$. One putative pathway is

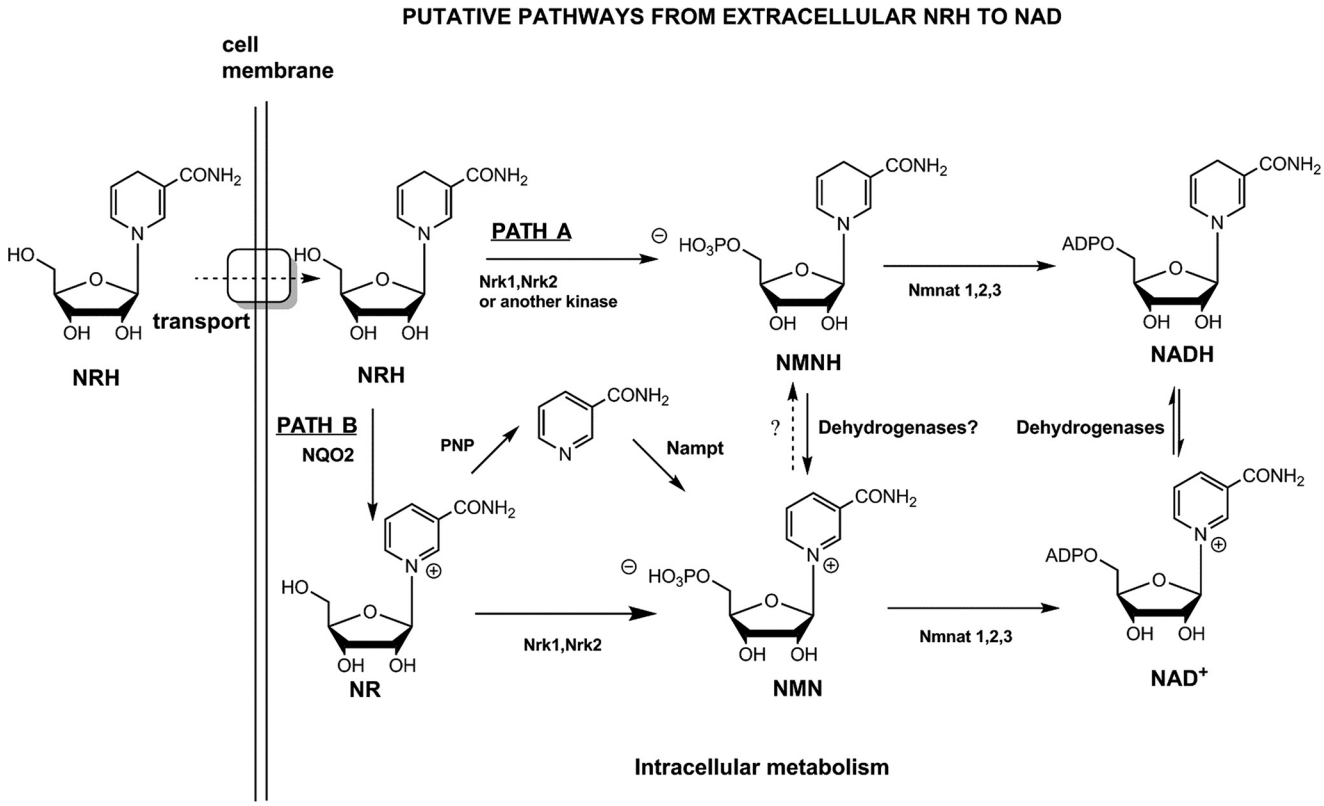

Figure 5. Illustration of putative pathways from extracellular NRH to NAD$^+$. NRH may be internalized via an unknown transporter as intact molecule and then is either directly phosphorylated (Path A) or oxidized to NR (Path B). Phosphorylation of NRH generates putative species NMNH (Path A), a putative intermediate, which would then be oxidized to NMN or further metabolized by nicotinamide mononucleotide adenylyltransferase 1 (Nmnat1), Nmnat2, or Nmnat3 to produce NADH and then converge on NAD$^+$.

nicotinamide salvage. To investigate this pathway as a possible player in NRH effects, we treated cells with FK866 (31), a known inhibitor of the enzyme nicotinamide phosphoribosyltransferase (Nampt), which is responsible for NAM recycling to NMN (32). FK866 causes depletion of NAD$^+$ concentrations in both HEK293 (Fig. 4*b*) and Neuro2a (Fig. 4*b*) cells. Decline in NAD$^+$ is attributable to failure of released NAM to be resynthesized into NAD$^+$. Co-administration of NRH with FK866 completely rescues the effect of FK866 on cells. Moreover, FK866 has no effect on NRH-induced NAD$^+$ increase. Thus, NRH-induced NAD$^+$ concentration increases do not apparently require nicotinamide recycling for the effect. Similarly, NR increased NAD$^+$ concentrations, and this effect was not very sensitive to FK866 (Fig. 4*b*), consistent with the interpretation that NR utilizes a kinase-dependent pathway independent of Nampt to provide the majority of its NAD$^+$ biosynthesis. Thus, NRH causes marked NAD$^+$ increases even when Nampt is inhibited, indicating a nicotinamide-independent and Nampt-independent mechanism of action.

Next, we asked whether it is possible that cells possess an activity that can convert NRH to a subsequent product, which could be on the biosynthetic pathway to NAD$^+$. We thus treated Neuro2a cell lysates with ATP (2 mM) and NRH (100 μM) and monitored for formation of product. We found that in the absence of ATP, no reaction of NRH was observed (data not shown), but in the presence of ATP, a new product was formed, of identical retention time to the compound dihydronicotinamide mononucleotide (Fig. 4*c*, NMNH; prepared by degradation of NADH with snake venom diesterase). To our knowledge, this conversion of NRH to NMNH (Fig. 4*c*, Neuro2a lysate at 37 °C; specific activity = 0.38 ± 0.05 pmol/min/μg protein; see Fig. 5 for structure of NMNH) has not previously been reported for cell lysates and provides a putative first metabolic step of NRH to NAD$^+$.

One possible mechanism for the conversion of NRH to NMNH could be action of known NR-dependent kinases, Nrk1 and/or Nrk2. To ascertain whether NRH induction of NAD$^+$ accumulation in cells requires Nrk1, we obtained HAP1 WT and Nrk1 KO cell lines (see "Experimental procedures") and prepared protein lysates from these cell lines. With these lysates, we measured NR kinase activity by measurement of [*carbonyl*-^{14}C]NR conversion to [*carbonyl*-^{14}C]NMN in the presence of ATP. Conversion of NR to NMN in WT HAP1 lysate was easily measureable, but this activity was completely lost in corresponding Nrk1 KO lysate (Fig. 4*d*). However, both WT and Nrk1 KO lysates retained NRH kinase activity, as shown by formation of NMNH in the presence of ATP (Fig. 4*e*). The biological activity of Nrk1 is known to regulate NR conversion to NAD$^+$ in some cell lines. In HAP1, this also appears to be the case. HAP1 WT cells have a statistically significant increase in NAD$^+$ concentrations when treated with NR, increasing to 190% of untreated control, whereas the corresponding Nrk1 KO shows no effect for NR in increasing NAD$^+$ content (Fig. 4*f*). Thus, Nrk1 is required for NR-induced NAD$^+$ increase in this cell line. On the other hand, WT and Nrk1 KO cell lines are both able to respond to NRH treatment, increasing

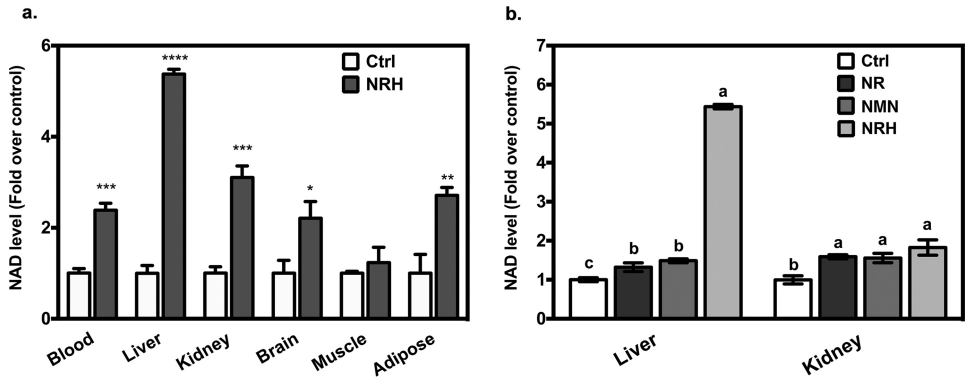

Figure 6. NRH increased tissue NAD$^+$ content *in vivo*. *a*, after intraperitoneal injection of 1000 mg/kg NRH in male C57BL/6J mice for 4 h, NAD$^+$ content in blood, liver, kidney, brain, and epididymal adipose tissue was increased compared with the control group. Data are shown as mean ± S.E. (*error bars*) ($n = 4$). *, $p < 0.05$; **, $p < 0.01$; ***, $p < 0.001$; ****, $p < 0.0001$ when compared with control. *b*, male C57BL/6J mice were intraperitoneally injected with one of 250 mg/kg NRH, 250 mg/kg NMN, 250 mg/kg NR, or vehicle and then sacrificed at 4 h. Liver and kidney NAD$^+$ content were compared across groups. Data are presented as mean ± S.E. ($n = 4$). *Different letters* indicate significant difference ($p < 0.05$) between groups.

6.8-fold over untreated controls (Fig. 4*f*). This result confirms that Nrk1 is not required for NRH conversion to NAD$^+$, consistent with results showing Nrk1 is also not required for conversion of NRH to NMNH (Fig. 4*e*).

Finally, we investigated whether recombinant Nrk2 could phosphorylate NRH and found that despite changes in pH from pH 7 to 9, recombinant Nrk2 could not measurably phosphorylate NRH (rate $<0.005\ s^{-1}$) to the extent observed by Neuro2a lysate (Fig. 4*g*). On the other hand, using [*carbonyl*-^{14}C]NR as a substrate, recombinant Nrk2 was clearly very active, exhibiting an observed rate of 3.07 s^{-1} under the same reaction conditions. Collectively, these experiments indicate that NRH is phosphorylated by a kinase not previously recognized to participate in NAD$^+$ metabolism to convert to it to NMNH. Moreover, NRH effects on NAD$^+$ concentrations appear to be independent of Nrk1 and Nrk2. These results lead us to propose that Path A (with elimination of Nrk1 or Nrk2 as possible kinases) depicted in Fig. 5 likely accounts for the majority of biological action of NRH and that Path B is not required for NRH effects on NAD$^+$ concentrations.

NRH in vivo

Finally, to assess biological effects in mice, we treated C57BL/6J mice by intraperitoneal injection with 1000 mg/kg NRH and assessed NAD$^+$ contents in tissues at 4 h. As can be observed in Fig. 6, NAD$^+$ contents increased severalfold in blood, brain, adipose, and kidney, with a greater than 5-fold increase in liver NAD$^+$ concentrations at 4 h (Fig. 5*a*). The weakest effects were observed in skeletal muscle, where increases were above control but not statistically significant. Table 1 shows measured NAD$^+$ contents and observed errors. As shown by the data, NRH is an effective NAD$^+$ concentration enhancer in many animal tissues and organs upon single dose administration. To assess for possible perturbation of redox potential, we measured NADH content in liver, which is the most profoundly affected organ with NRH treatment. We determined a NAD/NADH ratio of 68 ± 10 in NRH-treated liver.

To determine whether NRH is more effective than other NAD$^+$ precursors *in vivo*, we injected 250-mg/kg intraperitoneal doses of NRH, NMN, NR, or vehicle only and measured

Table 1
Tissue NAD$^+$ values in control and NRH-treated C57BL/6J mice
Data are presented as mean ± S.E.

Tissue	NAD$^+$ concentration	
	Control	NRH
	pmol/mg	
Blood	23.9 ± 2.2	57.0 ± 4.6
Liver	834.9 ± 130.7	4488.1 ± 142.0
Kidney	590.8 ± 83.9	1833.1 ± 148.9
Brain	51.0 ± 13.5	112.9 ± 17.3
Muscle	274.3 ± 11.6	338.3 ± 91.9
Adipose	15.2 ± 5.9	41.3 ± 2.7

NAD$^+$ contents in kidney and liver at 4 h (Fig. 5*b*). We found that in kidney NR, NRH and NMN statistically increased NAD$^+$ contents above control, with NRH providing the highest effect at 180% with NR and NMN providing 159 and 156%, respectively. In liver, NRH increased NAD concentration by 540%, whereas NR and NMN provided 132 and 149%, respectively (Fig. 5*b*). Thus, NRH provides larger NAD$^+$ increases than NR and NMN at equivalent doses and in liver provides quite significant NAD$^+$ increase at a low dose, consistent with improved pharmacologic potency *versus* other NAD$^+$ precursors. These findings recapitulate observations made with cell culture studies.

Discussion

The discovery of novel agents to increase cellular NAD$^+$ is of recent high interest in the biomedical research community, with a number of ongoing clinical studies and several recent published ones involving the newly discovered NAD$^+$-enhancing agents NR and NMN (18, 19). In the current work, the previously uninvestigated compound NRH was synthesized and was determined to be a potent and effective enhancer of NAD$^+$ concentrations in cultured cells as well as primary neurons. The maximal concentration enhancements were manyfold over control values and reached unprecedented levels of up to 10-fold in Neuro2a cells and over 7-fold in cultured primary neurons. These effects raise the bar for a pharmacological agent of this kind. NRH was found to exceed NR and NMN effects by several- to manyfold in this respect, suggesting a unique mechanism of action. Moreover, in terms of potency, NRH achieved a 260% NAD$^+$ concentration *versus* control in Neuro2a cells at

34 μM, whereas NR required 1 mM for this same effect (17), indicating that NRH is ~30 times more potent than NR under these conditions. Similar doubling of NAD$^+$ concentrations occurred at NRH concentrations below 100 μM in primary neurons.

NRH has NAD$^+$ concentration enhancement effects requiring 1–6 h to occur in cell culture, and its effects can remain sustained for up to 18 h. Effects reaching doubling of NAD$^+$ concentrations occurred in as little as 1 h (Fig. 2*d*). Time courses for the effects of NAD$^+$ precursors on intracellular NAD$^+$ concentrations have remained largely unreported. Dose-response profiles of NRH in both Neuro2a cells and primary neurons indicate EC_{50} values (defined in the legend of Fig. 2) between 100 and 300 μM, indicating a large dynamic concentration range for NRH action. Cell culture studies in at least eight cell lines showed that NRH was also able to substantially raise NAD$^+$ concentrations, and this activity of NRH was also observed *in vivo*. NRH injected by intraperitoneal administration increased NAD$^+$ concentrations manyfold in a variety of mouse tissues (Table 1). The dose-response profile for NRH in mice or any other animal remains to be established and is an objective of future research in the laboratory.

A concern with pharmacologic use of NAD$^+$ concentration enhancers is the prospect that they may cause an undesired cell toxicity or cause perturbations to NAD$^+$/NADH ratio. Cell counts were slightly decreased in HEK293 cells in 24-h incubations as determined by cell counts, but there was no evidence for activation of apoptosis. Moreover, the NAD$^+$/NADH ratio was markedly changed. NRH treatment after 6 h caused marked increases in NAD$^+$ accumulation in cultured cells but less pronounced increases to NADH concentrations. Consequently, the accumulation of NAD$^+$ shifts the NAD$^+$/NADH ratio higher and suggests a strong homeostasis that keeps NADH concentrations relatively lower. At the highest dosage tested, NAD$^+$/NADH ratio in liver was increased to 68 ± 10 with NRH treatment. Prior reports in the literature for mouse liver NAD$^+$/NADH range from 1 to 10 (33) and in rat liver from about 2 to 8 (29). However, in rat liver, free NAD$^+$/NADH is in the range 10–700 depending on whether cytoplasm or mitochondria is measured (29). We speculate that the higher NAD$^+$/NADH ratio with NRH treatment is likely due to shifting the ratio toward the protein-unbound NAD$^+$/NADH ratio which is typically much higher than the protein-bound ratio (29). This effect could be a consequence of saturation of protein-binding sites for NAD$^+$ and NADH in liver at higher NAD$^+$ concentrations, causing the overall ratio to move higher. The ramifications of consistent increase of the NAD$^+$/NADH ratio in cells and tissues is an open question, although arguably it poises cells to become more oxidative and may increase metabolic capacity.

Increasing cellular NAD$^+$ pools by up to 10-fold suggests that NRH could compensate NAD$^+$ depletion caused by genotoxic stress. Cells treated with either peroxide or the alkylative genotoxin MMS were depleted of cellular NAD$^+$ and experienced cell death. In contrast, cells treated with toxin and NRH maintained higher NAD$^+$ concentrations and experienced increased cell survival. These studies provide proof of concept for NRH as a cellular NAD$^+$ protection agent and cell survival agent. Differences in cell responses to the two treatments appear to arise from lifetimes of MMS and HP in medium in the presence of cells. MMS is persistent in medium, and cells have depleted NAD$^+$ even after 6 h of treatment. HP-treated cells experience rapid depletion of HP in medium, leading to recovery in NAD$^+$ homeostasis at 6 h. Nevertheless, NRH is effective in protection of cell NAD$^+$ and cell viability in both genotoxic treatments and is more effective than NR in HEK293 in peroxide treatments (Fig. 3*c*) and Neuro2a cells in MMS treatments (Fig. 3*f*).

To our knowledge, previous research had not investigated NRH as an NAD$^+$ precursor, and prior work had only uncovered a substrate role for NRH in the action of NQO2 (34). The biogenic origin of NRH in cells and tissues is currently unknown, and its occurrence in mammalian cells is also undocumented. One possible downstream metabolic fate of NRH is conversion to NMNH, as demonstrated in cell lysates in this report. Studies to understand how NRH augments cellular NAD$^+$ concentrations revealed that it is probably not inhibiting NAD$^+$ consumption. This was investigated by measurement of loss of [*carbonyl*-^{14}C]NAD$^+$ in Neuro2a cells treated with NRH or with vehicle. In fact, NRH-treated cells had increased NAD$^+$ turnover, and this is likely because increased NAD$^+$ concentrations drive increased cellular demand for NAD$^+$. The specific origin of this increased demand for NAD$^+$ is unclear, but it could be due to sub-saturation of enzymes that consume NAD$^+$ as a substrate. This idea has been postulated to account for the actions of NAD$^+$ precursors as drivers of cellular adaptation.

Consequently, the simplest explanation of NRH effects on NAD$^+$ concentration is that it acts as a biosynthetic precursor to NAD$^+$ via very efficient biosynthetic pathways. Fig. 5 presents likely metabolic pathways emanating from extracellular NRH and converging upon NAD$^+$. Although it is possible NRH is converted outside of cells to another species, we consider it unlikely that oxidation to NR or further breakdown to nicotinamide is responsible for NRH action, because neither NR nor nicotinamide alone provides the NAD$^+$ concentration enhancement effects observed for NRH. Moreover, breakdown of NRH to nicotinamide in either extracellular or intracellular compartments is apparently not required for NRH effects. This can be inferred from lack of effect of FK866, a potent inhibitor of Nampt and nicotinamide recycling. It had no effect on NAD$^+$ concentration increases induced by NRH.

We hypothesize that NRH encountering cell membranes is internalized, via an unknown transporter, or transporters and is internalized intact as NRH (Fig. 5). NRH is then acted upon by a kinase that converts NRH to a putative species NMNH (Path A). We showed that cell lysates possess an ATP-dependent activity capable of converting NRH to NMNH. The identity of this kinase is not Nrk1, as shown by the use of HAP1 WT and HAP1 Nrk1 KO cells. KO cells lack the ability to phosphorylate NR and to respond to NR in NAD$^+$ increase. However, HAP1 Nrk1 KO cells respond fully to NRH and respond equivalently to HAP1 WT cells. Moreover, we showed that recombinant Nrk2 cannot convert NRH to NMNH, although it can readily convert NR to NMN. The independence of NRH effects from Nrk1 activity implies that NRH is not acting as a precursor to

NR (Path B, Fig. 5) because Nrk1 regulates NR effects in HAP1 cells but is not required for NRH effects in this cell line. Moreover, there is virtually no remaining NR kinase activity in HAP1 Nrk1 KO cells as measured by activity assays (Fig. 4*d*), implying poor to nonexistent Nrk2 activity in this cell line. The current data indicate to us that an unidentified kinase is involved in the activity of NRH, acting most likely to form NMNH (Path A, Fig. 5), as demonstrated for HAP1 and Neuro2a lysates. The identification of this kinase and characterization of its role in NRH-mediated NAD^+ biosynthesis is an objective of future work by our laboratory.

In summary, these findings reveal a powerful naturally occurring pharmacologic agent that can raise NAD^+ levels in mammalian cells and tissues, providing an exceptional new tool to investigate how changes in NAD^+ metabolism can alter cellular physiology.

Experimental procedures

Synthesis of NRH (1-((2R,3S,4R,5R)-3,4-dihydroxy-5-(hydroxymethyl)THF-2-yl)-1,4-dihydropyridine-3-carboxamide)

In a flame-dried flask under an argon atmosphere, NR (100 mg, 0.24 mmol) was added to 10 ml of 50 mM potassium phosphate (pH 8.5) at 0 °C. After 5 min, 0.8 eq of sodium dithionate ($Na_2S_2O_4$) was added, and then the reaction was run at 0 °C for 30 min (progress of the reaction was monitored by HPLC; 70% of the starting material was consumed after 30 min). The crude product was purified by a C-18 column using water as eluent to obtain a light yellow solid. Yield was 70%.

Cell culture

HEK293, Neuro2a, F98, U87, LN229, and C2C12 cells were cultured in Dulbecco's modified Eagle's medium supplemented with 10% fetal bovine serum, 100 units/ml penicillin, and 100 μg/ml streptomycin. MIN6 cells were cultured in Dulbecco's modified Eagle's medium with 15% fetal bovine serum, 100 units/ml penicillin, and 100 μg/ml streptomycin. INS1 cells were maintained in Roswell Park Memorial Institute (RPMI)-1640 with 11.1 mmol/liter D-glucose supplemented with 10% fetal bovine serum, 100 units/ml penicillin, and 100 μg/ml streptomycin, 10 mmol/liter HEPES, 2 mmol/liter L-glutamine, 1 mmol/liter sodium pyruvate, and 50 μmol/liter 2-mercaptoethanol. Primary neurons were harvested from the brains of neonatal rats and plated overnight. Human nicotinamide riboside kinase (Nrk1) knockout HAP1 cell line and the corresponding WT HAP1 cells were purchased from Horizon Discovery (Cambridge, UK). HAP1 cells were cultured in Iscove's modified Dulbecco's medium with 10% fetal bovine serum, 100 units/ml penicillin, and 100 μg/ml streptomycin. Cells were maintained in a humidified incubator supplied with 5% CO_2, 95% air at 37 °C.

Identification of NRH and NAD^+ on HPLC

Samples containing NRH or NAD^+ were injected into an EC 250/4.6 Nucleosil 100-5 C18 column on a Hitachi Elite Lachrom HPLC system equipped with Diode Array Detector L-2450. The C18 column was eluted with 20 mM ammonium acetate at 1 ml/min for 25 min and then with 20 mM ammonium acetate and 20% methanol for 20 min. NRH was characterized by its peak at 340 nm, whereas NAD^+ was characterized by its peak at 260 nm.

Cellular NAD^+ measurement

For NAD^+ measurements, cells were seeded in 6-well plates until they reached ~90% confluence. Cells were treated with the desired concentrations of NRH or NR or NMN from concentrated stocks dissolved in water. Cells were harvested with trypsin digestion after treatment time. Unless indicated, the NRH treatment duration was 6 h. Cell numbers were counted using hemocytometer and trypan blue. The harvested cells were pelleted at 3000 × *g* for 3 min. After removing the remaining medium, cells were lysed with 7% perchloric acid to preserve NAD^+ and then neutralized with 2 M NaOH and 500 mM K_2HPO_4. The cellular NAD^+ levels were measured as published previously (27).

NADH measurement

To measure intracellular NADH levels, cell pellets were harvested after NRH treatment as described previously; lysed in 0.1 M NaOH, 1 mM EDTA; and then incubated at 80 °C for 10 min to avoid NAD^+ contamination. The samples were then neutralized with 0.5 M HCl and 500 mM KH_2PO_4. The NADH levels were measured as published (27).

Mitochondrial isolation

To measure the individual NAD^+ concentration in mitochondria, Neuro2a cells were seeded in a 10-cm^2 Petri dish and then treated with 1 mM NRH overnight. The cells were harvested with trypsin and pelleted by spinning at 3000 × *g* for 5 min. The mitochondrial fractions were isolated using the Mitochondrial Isolation Kit for Mammalian Cells (Thermo Scientific) according to the manufacturer's manual. Protein concentrations were later measured using a Bradford assay for normalization. NAD^+ concentrations were measured as reported (27).

Hydrogen peroxide stability test

HP in growth medium was measured by a plate reader assay (Sigma-Aldrich Fluorimetric Hydrogen Peroxide Assay Kit MAK165). 100 μM HP was incubated with either HEK293 or Neuro2a cells, both at 80–90% confluence. Medium was aliquoted at 0, 10, 20, 30, 40, and 60 min and assayed by dilution into 96-well plates according to the manufacturer's instructions. Curve fit of the points is to the equation, [peroxide] = A1 + A2·exp($-kt$), where k is the observed rate constant, $A1$ is the residual concentration of peroxide at infinite time, and $A2$ is the starting peroxide concentration. A standard curve was generated with known peroxide concentrations to achieve quantitation for the biological samples.

Methyl methanesulfonate stability test

Growth medium containing 1 mM MMS was incubated with 80% confluent HEK293 cells or Neuro2a cells in 6-well plates. At 0, 2, and 4 h, the concentration of MMS in medium was determined by mixing 50 μl of medium with 5 μl of 1 M nicotinamide. Samples were heated at 80 °C for 10 min. The reac-

tion was subsequently diluted with 200 μl of water and then injected onto a C-18 column on HPLC and eluted with 20 mM ammonium acetate followed by 20 mM ammonium acetate with 20% MeOH. *N*-Methylnicotinamide (260-nm detection) eluted before unreacted nicotinamide, and the peak area of *N*-methylnicotinamide was quantified. A standard curve with a range of MMS concentrations was obtained similarly to quantitate samples.

NAD$^+$ turnover

To measure the NAD$^+$ turnover rate in the presence or absence of NRH, Neuro2a cells were seeded into a 6-well plate until ~90% confluent and treated with 700,000 cpm of [^{14}C]NAM (Movarek Biochemicals) per well overnight. Cells were then washed with PBS twice and incubated with or without 1 mM NRH. Both medium and cells were harvested at 0, 1.5, 3, 5, and 7 h. Radioactivity of medium was directly counted by scintillation counter (Beckman Coulter). Cells were trypinsized and pelleted and then extracted with 7% perchloric acid and injected onto HPLC. The NAD$^+$ peak was collected using the above mentioned elution system and counted for radioactivity.

FK866 effect on NAD$^+$ levels

To understand the effects of nicotinamide recycling on NRH action, Neuro2a and HEK293 cells were treated with vehicle or 20 nM FK866, an NAMPT inhibitor that blocks the synthesis of NMN from nicotinamide. Additional added components included vehicle, 1 mM NR, or 1 mM NRH. Cells were harvested after 6 h, and NAD$^+$ was measured as described previously (27).

Identification of NMNH on HPLC

To measure NRH kinase activity, 100 μM NRH, 2 mM ATP, and 5 mM Mg^{2+} were combined with Neuro2a protein lysate (122 μg of protein), all prepared in 100 μl of radioimmune precipitation assay buffer (Amresco, catalog no. 653, 100 ml). Reactions were incubated for 30 min at 37 °C. Corresponding controls with no lysate or no ATP were also incubated. The reactions were then ceased by incubating at 60 °C for 2 min and then spun by microcentrifuge at maximum speed for 10 min at 4 °C to remove precipitated protein. Supernatant was injected onto a C-18 column on an HPLC system and eluted with 20 mM ammonium acetate. The conversion of NRH to NMNH was characterized by integration of peaks with detection wavelength of 340 nm. Authentic NMNH was prepared by digestion of NADH with snake venom diesterase. Authentic NMNH was used as a chromatographic standard.

Synthesis of ^{14}C-labeled NR

To test NR phosphorylation activity of enzymes, [*carbonyl*-^{14}C]NR was prepared from [*carbonyl*-^{14}C]NAM (Moravek Biochemicals). First, 5 μCi of radioactive NAM was added to 1 mM unlabeled NAM, 600 μM NAD$^+$, and 200 μM acetylated peptide JB12 (Rockefeller University Proteomics Resource Center) in the presence of 1 μM recombinant SirT1 protein in 100 μl of 20 mM KH_2PO_4, pH 7. Reaction was incubated at 37 °C for 1 h and then quenched with 5% TFA. The [*carbonyl*-^{14}C]NAD$^+$ product was purified by injection onto a C-18 column on HPLC eluted with 0.1% TFA at 1 ml/min for 25 min and then with 0.1% TFA and 20% MeOH for 20 min. The fraction containing [*carbonyl*-^{14}C]NAD$^+$ was dried by vacuum. [*carbonyl*-^{14}C]NAD$^+$ dissolved in 100 μl of 20 mM KH_2PO_4, pH 7, and treated with snake venom diesterase and alkaline phosphatase at 37 °C for 2 h. The reaction was quenched by the addition of 5% TFA. The resulting [*carbonyl*-^{14}C]NR was purified by injection onto a C-18 column on HPLC and collected and dried, similar to the procedure described above. The concentration of [*carbonyl*-^{14}C]NR was determined by peak area and compared with an authentic weighed NR standard. Specific activity was determined by scintillation counting of a known amount of [*carbonyl*-^{14}C]NR.

HAP1 cell lysate activity test

Human Nrk1 sequence was disrupted in the HAP1 cell line by a 1-bp insertion in exon 5 of transcript NM_017881 by Horizon Discovery, and the mutation was validated by the sequencing result by the company. Protein lysates from WT and human Nrk1 knockout HAP1 cells were extracted with radioimmune precipitation assay buffer and quantified by a Bradford assay. To test the lysate activity against NR, equal protein masses of WT and Nrk1 knockout HAP1 lysates were incubated with 100 μM NR containing 8000 cpm of [*carbonyl*-^{14}C]NR, 2 mM ATP, 5 mM Mg^{2+}, and 150 mM KH_2PO_4 at pH 7. After incubation at 37 °C for 30 min, the reactions were quenched by adding a 10% volume of 20% TFA and incubated on ice for 5 min. [*carbonyl*-^{14}C]NMN and [*carbonyl*-^{14}C]NR were collected after injection onto a C-18 column on HPLC eluted with 20 mM ammonium acetate and 20% MeOH. Fractions containing NMN and NR were counted separately by a scintillation counter. To test the lysate activity against NRH, equal masses of cell lysates were incubated with 2 mM NRH, 2 mM ATP, 5 mM Mg^{2+}, and 150 mM KH_2PO_4 at pH 9 at 37 °C for 30 min. The protein in the reaction was removed by passing the reaction mixture through a 10K Amicon Ultra centrifugal filter (Millipore). NMNH was identified at 340 nm using the HPLC system mentioned above.

Human Nrk2 protein cloning and activity test

Human Nrk2 sequence (NM_017881.2) was cloned into a pET28a plasmid and sequenced. The plasmid was transfected into BL21-Codon Plus cells (catalog no. 230280, Agilent Technologies) for protein expression. Induction of cultures at A_{600} = 0.5 at 37 °C was followed by 4 h of continued growth, followed by centrifugation to pellet. Pellets were resuspended in 75 mM KH_2PO_4, pH 7 (5 volumes), and lysozyme and DNase were added to break cells and digest DNA. After three freeze-thaw cycles, lysates were clarified by centrifugation and added to nickel-agarose. His-tagged Nrk2 protein was eluted with 250 mM imidazole, 75 mM KH_2PO_4, 200 mM NaCl, pH 7.0. A Bradford assay and silver staining were used to quantify the protein concentration and to visualize the purity of protein. Protein was combined with 15% glycerol, 1 mM DTT and frozen in aliquots at −80 °C until use. To determine protein activity, 100 nM Nrk2 protein was incubated with 500 μM NR, 5 mM Mg^{2+}, 2 mM ATP including 8000 cpm of [*carbonyl*-^{14}C]NR in the presence of 150 mM KH_2PO_4 at pH 7, 37 °C for 1 h. NMN and NR were separated by HPLC and counted by a scintillation counter for ^{14}C activity. For activity with NRH, assays were performed as above,

except that pH was varied from 7 to 9. No NR was added, and 1 mM NRH was used, and reactions were monitored by HPLC as described previously.

NRH effects on NAD+ in vivo

Eight male C57BL/6J mice at 8 weeks old were purchased from Charles River and were housed in a polycarbonate cage under a 12-h light/dark cycle with free access to food and water. Then the mice were randomly assigned to two groups and received an intraperitoneal injection of either 1000 mg/kg NRH dissolved in PBS or only PBS in the control group. After 4 h, these mice were subjected to cardiac puncture for blood collection and sacrificed. Blood was collected into tubes containing EDTA (BD Vacutainer) and centrifuged for 20 min at 5000 × *g* at 4 °C, and then plasma was collected and stored at −80 °C. Liver, kidney, brain, muscle, and epididymal adipose tissue were harvested, immediately frozen in liquid nitrogen, and then stored at −80 °C until NAD^+ analyses. To understand the effect of NRH compared with NMN and NR at a lower dosage, a similar experiment was done with intraperitoneal injection of one of the following: 250 mg/kg NRH, 250 mg/kg NR, or 250 mg/kg NMN, or PBS. Then the mice were sacrificed after 4 h for tissue collection. All procedures were approved by the Institutional Animal Care and Use Committee of Weill Cornell Medicine. For NAD^+ analysis, ~100 mg of frozen tissue was pulverized in liquid nitrogen and homogenized in 7% perchloric acid by sonication, and then the solution was neutralized and subjected to NAD^+ measurement as described above. For NADH measurement, ~100 mg of frozen tissue was pulverized in liquid nitrogen and homogenized in water by sonication and then heated at 80 °C for 2 min. The extractions were then centrifuged and injected onto HPLC. NADH peak was quantified at 340 nm, and the concentration was determined by an NADH standard.

Author contributions—Y. Y. and A. A. S. conceptualization; Y. Y. investigation; Y. Y. and A. A. S. writing-original draft; Y. Y. and A. A. S. writing-review and editing; N. Z. and A. A. S. methodology; A. A. S. funding acquisition; F. S. M. synthesis.

References

1. Yang, Y., and Sauve, A. A. (2016) NAD^+ metabolism: bioenergetics, signaling and manipulation for therapy. *Biochim. Biophys. Acta* **1864,** 1787–1800 CrossRef Medline
2. Belenky, P., Bogan, K. L., and Brenner, C. (2007) NAD^+ metabolism in health and disease. *Trends Biochem. Sci.* **32,** 12–19 CrossRef Medline
3. Cantó, C., Menzies, K. J., and Auwerx, J. (2015) NAD^+ metabolism and the control of energy homeostasis: a balancing act between mitochondria and the nucleus. *Cell Metabol.* **22,** 31–53 CrossRef Medline
4. Hassa, P. O., Haenni, S. S., Elser, M., and Hottiger, M. O. (2006) Nuclear ADP-ribosylation reactions in mammalian cells: where are we today and where are we going? *Microbiol. Mol. Biol. Rev.* **70,** 789–829 CrossRef Medline
5. Yang, H., Yang, T., Baur, J. A., Perez, E., Matsui, T., Carmona, J. J., Lamming, D. W., Souza-Pinto, N. C., Bohr, V. A., Rosenzweig, A., de Cabo, R., Sauve, A. A., and Sinclair, D. A. (2007) Nutrient-sensitive mitochondrial NAD^+ levels dictate cell survival. *Cell* **130,** 1095–1107 CrossRef Medline
6. Katsyuba, E., and Auwerx, J. (2017) Modulating NAD^+ metabolism, from bench to bedside. *EMBO J.* **36,** 2670–2683 CrossRef Medline
7. Sauve, A. A. (2008) NAD^+ and vitamin B3: from metabolism to therapies. *J. Pharmacol. Exp. Ther.* **324,** 883–893 Medline
8. Scheibye-Knudsen, M., Mitchell, S. J., Fang, E. F., Iyama, T., Ward, T., Wang, J., Dunn, C. A., Singh, N., Veith, S., Hasan-Olive, M. M., Mangerich, A., Wilson, M. A., Mattson, M. P., Bergersen, L. H., Cogger, V. C., *et al.* (2014) A high-fat diet and NAD^+ activate Sirt1 to rescue premature aging in cockayne syndrome. *Cell Metab.* **20,** 840–855 CrossRef Medline
9. Zhu, X. H., Lu, M., Lee, B. Y., Ugurbil, K., and Chen, W. (2015) *In vivo* NAD assay reveals the intracellular NAD contents and redox state in healthy human brain and their age dependences. *Proc. Natl. Acad. Sci. U.S.A.* **112,** 2876–2881 CrossRef Medline
10. Verdin, E. (2015) NAD^+ in aging, metabolism, and neurodegeneration. *Science* **350,** 1208–1213 CrossRef Medline
11. Mouchiroud, L., Houtkooper, R. H., and Auwerx, J. (2013) NAD^+ metabolism: a therapeutic target for age-related metabolic disease. *Crit. Rev. Biochem. Mol. Biol.* **48,** 397–408 CrossRef Medline
12. Ryu, D., Zhang, H., Ropelle, E. R., Sorrentino, V., Mázala, D. A., Mouchiroud, L., Marshall, P. L., Campbell, M. D., Ali, A. S., Knowels, G. M., Bellemin, S., Iyer, S. R., Wang, X., Gariani, K., Sauve, A. A., *et al.* (2016) NAD^+ repletion improves muscle function in muscular dystrophy and counters global PARylation. *Sci. Transl. Med.* **8,** 361ra139 CrossRef Medline
13. Gariani, K., Menzies, K. J., Ryu, D., Wegner, C. J., Wang, X., Ropelle, E. R., Moullan, N., Zhang, H., Perino, A., Lemos, V., Kim, B., Park, Y. K., Piersigilli, A., Pham, T. X., Yang, Y., *et al.* (2016) Eliciting the mitochondrial unfolded protein response by nicotinamide adenine dinucleotide repletion reverses fatty liver disease in mice. *Hepatology* **63,** 1190–1204 CrossRef Medline
14. Cantó, C., Houtkooper, R. H., Pirinen, E., Youn, D. Y., Oosterveer, M. H., Cen, Y., Fernandez-Marcos, P. J., Yamamoto, H., Andreux, P. A., Cettour-Rose, P., Gademann, K., Rinsch, C., Schoonjans, K., Sauve, A. A., and Auwerx, J. (2012) The NAD^+ precursor nicotinamide riboside enhances oxidative metabolism and protects against high-fat diet-induced obesity. *Cell Metab.* **15,** 838–847 CrossRef Medline
15. Langley, B., and Sauve, A. (2013) Sirtuin deacetylases as therapeutic targets in the nervous system. *Neurotherapeutics* **10,** 605–620 CrossRef Medline
16. Qin, W., Yang, T., Ho, L., Zhao, Z., Wang, J., Chen, L., Zhao, W., Thiyagarajan, M., MacGrogan, D., Rodgers, J. T., Puigserver, P., Sadoshima, J., Deng, H., Pedrini, S., Gandy, S., Sauve, A. A., and Pasinetti, G. M. (2006) Neuronal SIRT1 activation as a novel mechanism underlying the prevention of Alzheimer disease amyloid neuropathology by calorie restriction. *J. Biol. Chem.* **281,** 21745–21754 CrossRef Medline
17. Yang, T., Chan, N. Y., and Sauve, A. A. (2007) Syntheses of nicotinamide riboside and derivatives: effective agents for increasing nicotinamide adenine dinucleotide concentrations in mammalian cells. *J. Med. Chem.* **50,** 6458–6461 CrossRef Medline
18. Yoshino, J., Baur, J. A., and Imai, S. I. (2018) NAD^+ intermediates: the biology and therapeutic potential of NMN and NR. *Cell Metab.* **27,** 513–528 CrossRef Medline
19. Rajman, L., Chwalek, K., and Sinclair, D. A. (2018) Therapeutic potential of NAD-boosting molecules: the *in vivo* evidence. *Cell Metab.* **27,** 529–547 CrossRef Medline
20. Martens, C. R., Denman, B. A., Mazzo, M. R., Armstrong, M. L., Reisdorph, N., McQueen, M. B., Chonchol, M., and Seals, D. R. (2018) Chronic nicotinamide riboside supplementation is well-tolerated and elevates NAD^+ in healthy middle-aged and older adults. *Nat. Commun.* **9,** 1286 CrossRef Medline
21. Dellinger, R. W., Santos, S. R., Morris, M., Evans, M., Alminana, D., Guarente, L., and Marcotulli, E. (2017) Repeat dose NRPT (nicotinamide riboside and pterostilbene) increases NAD^+ levels in humans safely and sustainably: a randomized, double-blind, placebo-controlled study. *NPJ Aging Mech. Dis.* **3,** 17 CrossRef Medline
22. Trammell, S. A., Schmidt, M. S., Weidemann, B. J., Redpath, P., Jaksch, F., Dellinger, R. W., Li, Z., Abel, E. D., Migaud, M. E., and Brenner, C. (2016) Nicotinamide riboside is uniquely and orally bioavailable in mice and humans. *Nat. Commun.* **7,** 12948 CrossRef Medline
23. Gomes, A. P., Price, N. L., Ling, A. J., Moslehi, J. J., Montgomery, M. K., Rajman, L., White, J. P., Teodoro, J. S., Wrann, C. D., Hubbard, B. P., Mercken, E. M., Palmeira, C. M., de Cabo, R., Rolo, A. P., Turner, N., *et al.* (2013) Declining NAD^+ induces a pseudohypoxic state disrupting nucle-

ar-mitochondrial communication during aging. *Cell* **155,** 1624–1638 CrossRef Medline

24. Gong, B., Pan, Y., Vempati, P., Zhao, W., Knable, L., Ho, L., Wang, J., Sastre, M., Ono, K., Sauve, A. A., and Pasinetti, G. M. (2013) Nicotinamide riboside restores cognition through an upregulation of proliferator-activated receptor-γ coactivator 1α regulated β-secretase 1 degradation and mitochondrial gene expression in Alzheimer's mouse models. *Neurobiol. Aging* **34,** 1581–1588 CrossRef Medline
25. Riches, Z., Liu, Y., Berman, J. M., Walia, G., and Collier, A. C. (2017) The ontogeny and population variability of human hepatic dihydronicotinamide riboside:quinone oxidoreductase (NQO2). *J. Biochem. Mol. Toxicol.* **31** CrossRef Medline
26. Megarity, C. F., Gill, J. R., Caraher, M. C., Stratford, I. J., Nolan, K. A., and Timson, D. J. (2014) The two common polymorphic forms of human NRH-quinone oxidoreductase 2 (NQO2) have different biochemical properties. *FEBS Lett.* **588,** 1666–1672 CrossRef Medline
27. Li, W., and Sauve, A. A. (2015) NAD$^+$ content and its role in mitochondria. *Methods Mol. Biol.* **1241,** 39–48 CrossRef Medline
28. Brochier, C., Jones, J. I., Willis, D. E., and Langley, B. (2015) Poly(ADP-ribose) polymerase 1 is a novel target to promote axonal regeneration. *Proc. Natl. Acad. Sci. U.S.A.* **112,** 15220–15225 CrossRef Medline
29. Williamson, D. H., Lund, P., and Krebs, H. A. (1967) The redox state of free nicotinamide-adenine dinucleotide in the cytoplasm and mitochondria of rat liver. *Biochem. J.* **103,** 514–527 CrossRef Medline
30. Yang, T., and Sauve, A. A. (2006) NAD metabolism and sirtuins: metabolic regulation of protein deacetylation in stress and toxicity. *AAPS J.* **8,** E632–E643 CrossRef Medline
31. Hasmann, M., and Schemainda, I. (2003) FK866, a highly specific noncompetitive inhibitor of nicotinamide phosphoribosyltransferase, represents a novel mechanism for induction of tumor cell apoptosis. *Cancer Res.* **63,** 7436–7442 Medline
32. Wang, T., Zhang, X., Bheda, P., Revollo, J. R., Imai, S., and Wolberger, C. (2006) Structure of Nampt/PBEF/visfatin, a mammalian NAD$^+$ biosynthetic enzyme. *Nat. Struct. Mol. Biol.* **13,** 661–662 CrossRef Medline
33. Hayashida, S., Arimoto, A., Kuramoto, Y., Kozako, T., Honda, S., Shimeno, H., and Soeda, S. (2010) Fasting promotes the expression of SIRT1, an NAD$^+$-dependent protein deacetylase, via activation of PPARα in mice. *Mol. Cell. Biochem.* **339,** 285–292 CrossRef Medline
34. Wu, K., Knox, R., Sun, X. Z., Joseph, P., Jaiswal, A. K., Zhang, D., Deng, P. S., and Chen, S. (1997) Catalytic properties of NAD(P)H:quinone oxidoreductase-2 (NQO2), a dihydronicotinamide riboside dependent oxidoreductase. *Arch. Biochem. Biophys.* **347,** 221–228 CrossRef Medline